

Advances in Modeling Radiation Dispersal Device and Nuclear Detonation Effects

**J. S. Nasstrom, K.T. Foster, P. Goldstein, M. B. Dillon,
N. G. Wimer, S. Homann and G. Sugiyama**

Lawrence Livermore National Laboratory

PO Box 808, Livermore, CA 94551

nasstrom1@llnl.gov; foster3@llnl.gov; goldstein1@llnl.gov; dillon7@llnl.gov;
wimer1@llnl.gov; homann1@llnl.gov; sugiyama1@llnl.gov

ABSTRACT

Computer models that predict the effects of Radiation Dispersal Devices (RDD) and nuclear detonations are important tools for helping prepare for, and respond to, these threats. This paper describes recent advances made by Lawrence Livermore National Laboratory (LLNL) and collaborating laboratories in order to more realistically simulate (1) downwind deposition and dose from an RDD, (2) nuclear fallout fractionation processes, and (3) indoor radiation dose and sheltering strategies for nuclear fallout. These modeling capabilities are intended to produce near-real-time predictions to aid emergency preparedness and response by informing protective action decisions on sheltering, evacuation, relocation, and worker protection. These capabilities are developed for use in the Department of Energy (DOE) National Atmospheric Release Advisory Center (NARAC) at the LLNL, which also serves as the operations hub for the Department of Homeland Security led Interagency Modeling and Atmospheric Assessment Center (IMAAC).

Key Words: atmospheric dispersion modeling, radiation dispersal device, nuclear fallout

1 INTRODUCTION

Computer models of radioactive material dispersal are valuable tools for estimating dose and casualties resulting from nuclear accidents and terrorist threats, and for helping prepare for, and respond to, these threats. This paper describes recent advances in models used by the Department of Energy's National Atmospheric Release Advisory Center (NARAC) at Lawrence Livermore National Laboratory (LLNL). The NARAC modeling system utilizes real-time access to global meteorological data, geographical databases and 3-D meteorological and dispersion models [1] to produce real-time predictions as well as analyses of the impacts of atmospheric releases of hazardous materials. These models, as well as their testing and evaluation, have been described in previous publications [2].

The NARAC Lagrangian Operational Dispersion Integrator (LODI) code solves the 3-D advection-diffusion equation to simulate the processes of mean wind advection, turbulent diffusion, radionuclide decay and production, first-order chemical reactions, wet deposition, gravitational settling, dry deposition, and buoyant/momentum plume rise [2]. LODI is a Lagrangian Monte Carlo particle trajectory code that tracks marked fluid particles representing the release of contaminant into the atmosphere. An example LODI simulation for a hypothetical nuclear explosion is shown in Fig. 1.

The Atmospheric Data Assimilation and Parameterization Techniques (ADAPT) model [3] assimilates meteorological data from observations and/or weather forecast models, as well as

land-surface data, for use in LODI. ADAPT constructs meteorological fields (mean winds, pressure, precipitation, temperature, turbulence quantities, etc.) based on a variety of interpolation methods and atmospheric parameterizations. ADAPT produces non-divergent wind fields using an adjustment procedure based on the variational principle and a finite-element discretization. ADAPT can also ingest meteorological fields from high-resolution numerical weather prediction models, including output from an in-house version of the community Weather Research and Forecasting (WRF) model [4].

Due to uncertainties in modeling assumptions and input data under real-world conditions, the capacity to adjust predictions based on measurements of air and ground contamination is essential. The NARAC system can utilize sampling/monitoring data from field and aerial remote sensing teams provided by DOE and other agencies [5]. This allows predictions to be refined using measurement data, improving the accuracy of the predictions. The more accurate the models results, the better the fit that can be obtained to measurement results. In turn, NARAC model predictions are used as guidance for monitoring and sampling planning.

Recent modeling advances in NARAC models are described in this paper. Specifically, we discuss improvements to methods for predicting the explosive dispersal of radioactive material (Section 2), modeling of fractionation of fallout from nuclear explosions (Section 3), and estimation of dose from fallout to people sheltered indoors following a nuclear detonation (Section 4).

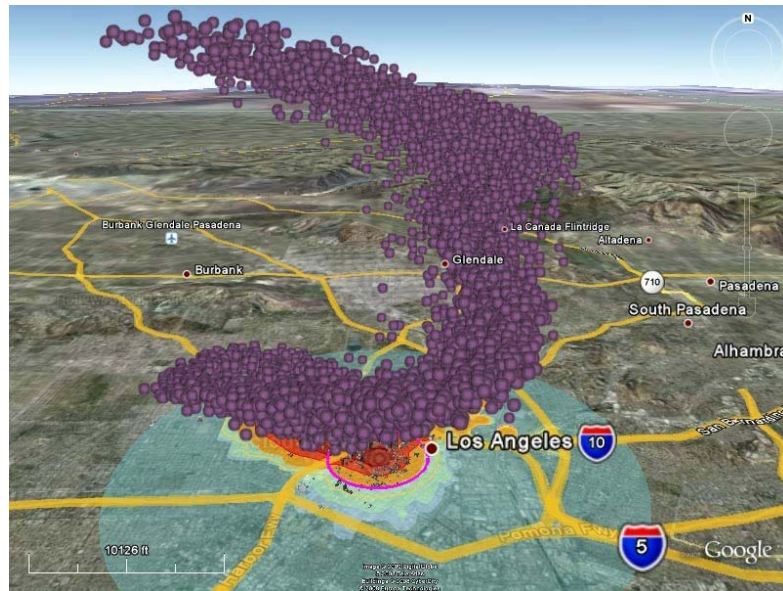


Figure 1. LODI marker particles several minutes after a hypothetical nuclear explosion. The concentric blue/green circles indicate different prompt damage levels centered on the detonation location and the edges of a two-lobed orange/red fallout pattern calculated by LODI are visible beneath the cloud of marker particles several minutes after detonation. Different wind transport directions are evident at different altitudes.

2 RDD BALLISTIC PARTICLE MODELING

DOE's National Nuclear Security Administration (NNSA) supported the development of improvements to radiological dispersal device (RDD) modeling in both the NARAC LODI 3-D dispersion and deposition model and the HotSpot fast field-portable dispersion and deposition software code [6], which is also maintained by NARAC/LLNL. Until recently, both LODI and HotSpot assumed that all of the radioactive particulate mass was influenced by the rising thermally-buoyant gas following a conventional explosion, with subsequent transport and diffusion of the material by the mean wind and turbulence. However, recent experimental results have shown that this is not always the case.

Over the last 25 years, extensive studies have been conducted at Sandia National Laboratories (SNL) to characterize the particulate material resulting from explosive detonations [7]. This work shows that RDD detonations can result in particles ranging in size from a few microns to a thousand microns, or more. These studies also indicate that particles larger than approximately 100 μm in aerodynamic diameter (AD) do not become entrained in the hot cloud of gases, but separate from the rising plume and follow ballistic trajectories independent of the buoyancy effects produced by the detonation. These larger particles typically fall to the surface within several tens to a few hundred meters of the detonation location.

In prior versions of the NARAC and HotSpot dispersion and deposition models, buoyant rise was assumed to affect these larger particles, leading to over-prediction of the rise of these larger particles, over-prediction of the mass deposited far downwind, and under-prediction of deposition closer to the detonation location. While more detailed modeling of ballistic motion and drag forces could be added to the atmospheric flow and dispersion models to correct this behavior, our recent work used a relatively simple, practical and efficient parameterization to describe the additional mass expected to be deposited near the source (by particles greater than 100 μm AD) and to remove this deposited mass from the airborne plume.

The parameterization was derived using the *ScatterMe* model that was developed by SNL in the course of investigating and interpreting ballistic particle deposition. This model uses a Monte Carlo method to sample a distribution of different particle sizes, initial velocities, elevations, azimuths, and separation distances. Initial conditions were assigned to particles which represent a large sample of potential ballistic motions under varying device configuration and meteorological conditions, and the landing location of each particle was calculated deterministically by numerical integration. As this calculation is more computationally intensive than is desired for rapid emergency response calculations, empirical fits of the *ScatterMe* results in the form of functions of the key input parameters were then developed for use in LODI and HotSpot.

For implementation into LODI, SNL developed an interface to the ballistic-particle deposition routine, allowing it to be called for an arbitrary particle size distribution (based on a user-specified array of input bin masses and their associated minimum and maximum diameters). Input data must be provided for wind direction and speed, the particle density, and explosive mass, as well as a predefined set of concentration sampling grid point locations for which the deposition mass is calculated. The downwind extent of the ballistic particle deposition region is dependent on the device configuration (primarily the amount of high-explosive and resulting particle size distribution) and meteorological conditions (primarily wind speed and direction as a function of altitude).

When applying the new method, mass from larger particles is deposited much closer to the detonation location, compared to the previous method. To illustrate the effect of the new ballistic particle methods, a calculation was made with the following assumptions:

- Source material = 1 kg total mass of Sr-90 (in equilibrium with Y-90)
- Log-normal particle mass-size distribution:
 - 10% of mass between 0.1 μm –10 μm ; AMAD¹ = 2 μm , SGD² = 3
 - 20% of mass between 10 μm –100 μm ; AMAD = 250 μm , SGD = 3
 - 70% of mass between 100 μm –1000 μm ; AMAD = 250 μm , SGD = 3
- High explosive mass = 50 pounds TNT
- Winds approximately 3 m/s near the detonation site blowing from the west

Table I and Figure 2 show that the change in the calculated ground-shine dose rate produced by the deposited material in rem/hr at 12 hours after detonation with and without the inclusion of the new method for modeling the ballistic trajectory of the larger particles. The expected decrease in downwind deposition of material is seen for the ballistic case, since 70% of the mass is associated with particles which now follow ballistic trajectories. The inner deposition contours cover a larger area, reflecting the increase in deposited material from the ballistic particles in the immediate vicinity of the detonation.

ScatterMe results were also implemented into the HotSpot model using compatible methods which reproduce the general deposition footprint extent and magnitude as calculated by the empirical fits derived for use in LODI.

Table I. Dimensions of predicted groundshine dose rate areas shown in Fig. 2 (a) and (b)

Contour level, inner to outer (rem/hr)	Extent in Fig. 2(a) (m)	Area in Fig. 2(a) (m ²)	Extent in Fig. 2(b) (m)	Area in Fig. 2(b) (m ²)
100	13.3	125	15.8	325
50	21.1	350	18.2	550
25	34.7	650	19.6	700
10	62.2	1,399	21.3	999
5	95.0	2,299	23.5	1,099

¹ Activity Median Aerodynamic Diameter

² Standard Geometric Deviation

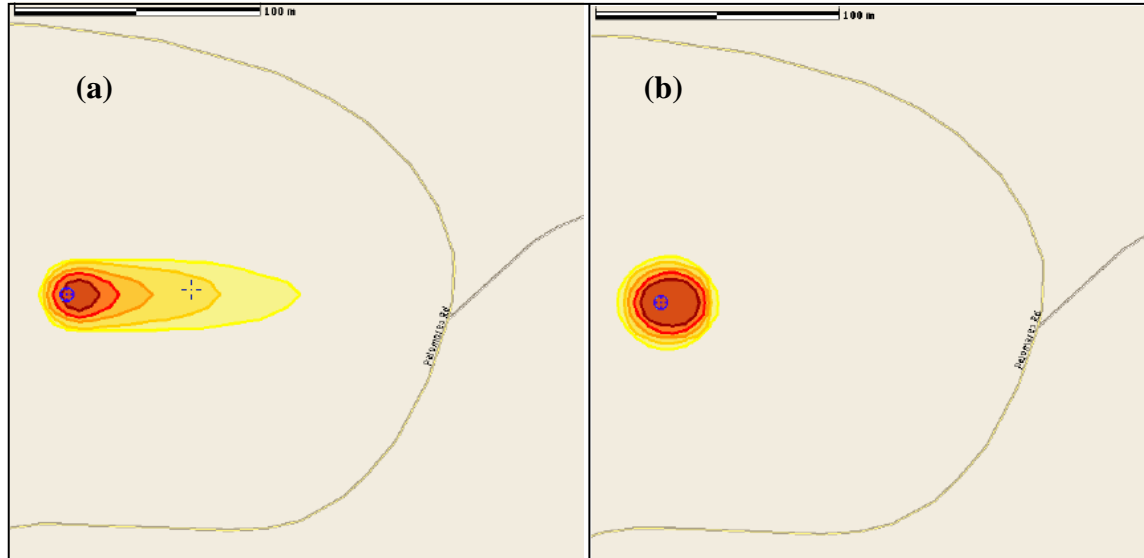


Figure 2. The LODI-calculated near-field ground-shine dose rate at 12 hours after detonation using (a) the original non-ballistic algorithms, and (b) the new ballistic trajectory parameterization. See Table I for legend.

3 FALLOUT FRACTIONATION MODELING

Accurate model predictions of fallout are needed to predict dose to the public and emergency response teams in order to protect their safety and health, and to assess environmental contamination. Fractionation is an important process following a nuclear detonation, as it causes volatile and refractory radionuclides to be deposited with significantly different proportions at different locations across the debris field. Therefore, tools to more accurately predict ground deposition – including radionuclide composition, and the distribution of refractory and volatile materials – need to account for fractionation.

Refractory radionuclides are those that form post-detonation chemical compounds that condense and solidify earlier (i.e., at higher temperatures) than the vaporized and liquefied carrier material (e.g., soil, rock). Because of this, refractory material becomes incorporated throughout the volume of carrier material particles as the nuclear fireball cools. In contrast, volatile radionuclides form chemical compounds that condense and solidify later, at lower temperatures, than the carrier material. As a result, volatile material is primarily incorporated on the surface of carrier material particles. Therefore, refractory and volatile material can have quite different activity-size distributions, as well as different settling and deposition rates.

DOE NNSA supported work to develop and implement fractionation modeling capabilities into NARAC's LODI model. We developed the new LODI model by implementing the radial power law activity-size distribution described by Freiling [8] and Tompkins [9], and by integrating it with other components of the existing LODI code. This approach has the advantage of being well established and tested.

Specifically, the new LODI code models fractionation according to the following calculation steps and features:

- a. Define the device total fission yield and component yields, and specific mass chains³ to be modeled, then use the Livermore Weapons Activation Code, LWAC, developed by Spriggs, et al. [10] to determine the initial ($t = 0$) radionuclide inventories (number of atoms)
- b. Use a Bateman equations solver to determine fission product inventories decayed forward to the carrier material solidification time as determined from time-temperature-yield relationships
- c. Determine the radionuclide constituents in each mass chain and identify each nuclide as either volatile or refractory at the solidification time, based on that radionuclide's oxide boiling points (the ratio of refractory atoms to total atoms in a mass chain is the Freiling ratio, Fr.)⁴
- d. Determine particle activity-size distributions (ASD) of the fission product decay mass chain by using a modified radial power law [8], based on the mean and standard deviation of the log normal particle number-size distribution for the carrier material and the Freiling ratio for the radionuclide mass chain
- e. Use a Bateman equations solver to obtain radionuclide inventories and the number of atoms in individual mass chains at the effective cloud-stabilization time, which is the LODI simulation start time (presently taken to be 10 minutes)
- f. Calculate the initial effective, static activity-height distribution, and dimensions of the debris cloud
- g. Using as input the device yield estimate, user specified meteorology, source location data, and fission product inventories, along with the Freiling ratios and activity-size distributions determined for each mass chain, run LODI to calculate the atmospheric transport, diffusion, settling and ground deposition, and obtain the atom concentration and deposition as specific abundances for each radionuclide across mass chains
- h. Compute fractionation ratios, r , as the ratio of the specific abundances for each selected mass chain divided by a reference mass chain specific abundance, for 2-D fallout fields and specific deposition points.

Initial model verification and validation of the LODI fractionation predictions have been conducted. The principal results of this work are summarized below:

- Model verification results are consistent with theory and assumptions. Results of the new model are consistent with theoretical relationships that describe the functional relationship between fractionation ratio pairs. The simulated correlation slopes agree with those expected from the radial power law model.

³ A mass chain is the chained series of parent and daughter radionuclides beginning with an original suite of fission product radionuclides and ending in a stable isotope. Since fission product decay chains involve primarily beta decay (neutron-to-proton transformation), radionuclides in a chain primarily have the same atomic mass number (e.g., I-131 and Xe-131), and the mass chain is identified by that atomic mass number (e.g., 131).

⁴ The Freiling ratio is ratio of the number of refractory atoms to total atoms in a mass chain at the solidification time of the carrier material. The Freiling ratio is used to control whether the radionuclide activity-size distribution is proportional to particle volume (for refractory radionuclides), particle surface area (for volatile radionuclides), or intermediate between volume and surface area (for mass chains with both volatile and refractory radionuclides). It is assumed that all radionuclides in a given mass chain are distributed on particles that transport and deposit together, and have the same particle activity-size distribution.

- Test model simulations show that fallout deposition levels of refractory radionuclides are higher close to the detonation location and fall off much more rapidly with distance, compared to volatile radionuclides, as expected, since refractory material tends to have relatively more activity on larger particles. Results show that volatile and refractory material fallout patterns can be significantly different in width and direction, due to differences in the settling rates and variation of wind speed and direction with altitude.
- Initial model validation was done using data from a U.S. nuclear above-ground test that provided measurements of fallout composition across the debris field. Model results show good agreement with near-field (less than 11 km downwind of ground zero) fallout measurements of refractory species and some volatile species. Further model-data comparisons are needed to develop insights into the model input data sensitivities, limitations of model accuracy, and reliability of fallout debris measurements.

4 SHELTERING EFFECTS

Sheltering is a standard strategy to reduce civilian population exposures. Accurate estimates of urban shielding are critical for realistic predictions of overall radiation exposures and casualties. Recently, the Department of Homeland Security has supported the development of capabilities that can be used to rapidly assess the quality of U.S. urban shelter quality following a nuclear detonation. Specifically, we have developed prototype tools that can be used to estimate: (a) the protection provided by existing buildings to fallout radiation, (b) the regional (neighborhood to city-scale) effectiveness for several shelter strategies that utilize these buildings, and (c) the indoor radiation exposures expected if these shelter strategies are used.

We have developed a capability that provides a “top-down” approach to estimating regional shelter effectiveness by combining national-level databases of building and population distributions with the protection expected for different types of buildings. The current capability produces maps of the regional distribution of fallout shelter quality and estimates of indoor radiation exposure (see Fig. 3) for the following three shelter strategies:

- Local Shelter: people obtain the best protection in the local area (e.g., a nearby concrete hospital)
- Shelter-in-Place: people obtain the best protection available in the building that they are in at the time of detonation (e.g., everyone shelters in the basement)
- No-Response: people do not move from their location within the building that they are in at the time of detonation (e.g., everyone in an office building remains seated at their desk).

A second capability provides a complementary “bottom-up” approach. First, a simple, fast-running screening tool (PFscreen) translates readily available local individual building data into building-specific radiation shielding estimates. Then, individual building estimates are combined to produce neighborhood-level estimates of the regional shelter quality and the effectiveness of various shelter strategies for this neighborhood is assessed. This new tool has tested well against a limited set of historical measurements and further refinement and testing is in progress.

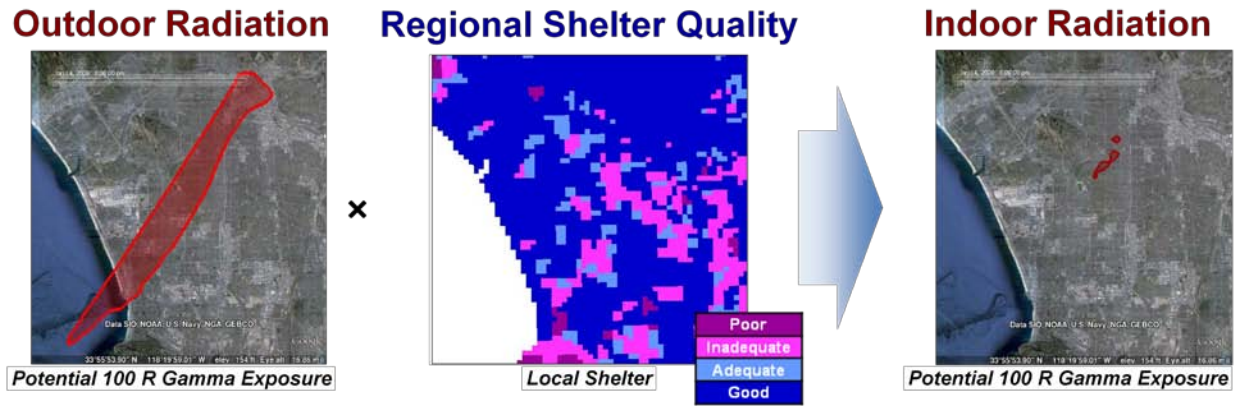


Figure 3. Example of a regional shelter quality assessment (center panel) and associated outdoor and indoor fallout radiation exposures for an illustrative scenario (left and right panels, respectively)

5 CONCLUSIONS

In this paper, we have described some recent improvements to modeling the dispersion and fallout of radioactive material from Radiation Dispersal Devices (RDD) and nuclear detonations. New methods for simulating larger, ballistic particles from an explosive RDD in the NARAC LODI and HotSpot models were shown to produce significantly larger near-field deposition and groundshine dose, compared to older methods that do not account for ballistic particles being quickly ejected from the buoyant cloud of rising gas. The addition of an approach to modeling the fractionation of nuclear explosion fallout in the LODI model shows promise for being able to predict the differences between volatile and refractory radionuclide deposition in fallout fields. A prototype capability was described that allows rapid assessment of the protection from fallout radiation that is provided by existing buildings. This capability can be used to generate databases of regional shelter quality which in turn can be used to evaluate the effectiveness of different sheltering strategies in order to inform life-saving decisions.

6 ACKNOWLEDGMENTS

Drs. Marv Larsen and Fred Harper from Sandia National Laboratories provided valuable help with ballistic particle modeling methods. The authors thank Drs. Gerard Garino and Dan Blumenthal from the Department of Energy (DOE) National Nuclear Security Administration (NNSA) for their valuable support of work on improved RDD modeling. The authors also thank Donald Daigler, Donald Lumpkins and Patricia Underwood from the Department of Homeland Security (DHS) for their support in developing the regional shelter assessment capability.

The authors gratefully acknowledge the assistance of Mr. Brooke Buddemeier, Dr. Jave Kane, Mr. David Price, Ms. Priya Doshi, Mr. Rich Belles, Mr. Hoyt Walker, Ms. Kathleen Fisher, Ms. Diane LaMartine, Mr. Miguel Castro, Mr. Eric Archibald, Ms. Erika Olsen, Dr. Matt Dombrowski and Dr. Lee Davidson at the LLNL; Dr. Larry Brandt at the Sandia National Laboratories; Dr. Richard Sextro at the Lawrence Berkeley National Laboratory; Mr. Steve Meheras at the Pacific Northwest National Laboratory; Mr. Philip Schneider at the National

Institute of Building Science; Mr. Dennis Schaeffer at the Science Applications International Corporation; Dr. Charles Kircher at Charles Kircher and Associates; Mr. David Montague at ABS Consulting; Mr. Neil Blais at Blais and Associates; and Ms. Hope Seligson at MMI Engineering.

This work performed under the auspices of the U.S. Department of Energy by Lawrence Livermore National Laboratory under Contract DE-AC52-07NA27344. The Department of Homeland Security sponsored part of the production of this material under the same contract.

7 DISCLAIMER

This document was prepared as an account of work sponsored by an agency of the United States government. Neither the United States government nor Lawrence Livermore National Security, LLC, nor any of their employees makes any warranty, expressed or implied, or assumes any legal liability or responsibility for the accuracy, completeness, or usefulness of any information, apparatus, product, or process disclosed, or represents that its use would not infringe privately owned rights. Reference herein to any specific commercial product, process, or service by trade name, trademark, manufacturer, or otherwise does not necessarily constitute or imply its endorsement, recommendation, or favoring by the United States government or Lawrence Livermore National Security, LLC. The views and opinions of authors expressed herein do not necessarily state or reflect those of the United States government or Lawrence Livermore National Security, LLC, and shall not be used for advertising or product endorsement purposes.

8 REFERENCES

1. Sugiyama, G., J.S. Nasstrom, R. Baskett, and M. Simpson, 2010: National Atmospheric Release Advisory Center (NARAC) Capabilities for Homeland Security, *5th International Symposium on Computational Wind Engineering*, Chapel Hill, NC May 23-27, 201
2. Nasstrom, J. S., G. Sugiyama, R. L. Baskett, S. C. Larsen, M. M. Bradley, 2007: The NARAC modeling and decision support system for radiological and nuclear emergency preparedness and response, *Int. J. Emergency Management*, **4**, 524-550
3. Sugiyama, G. and S. T. Chan, 1998: A New Meteorological Data Assimilation Model for Real-Time Emergency Response, Preprint, *10th Joint Conference on the Applications of Air Pollution Meteorology*, Phoenix, AZ (11-16 January, 1998), Am. Met. Soc., Boston, MA. 285-289
4. Simpson, M., V. Bulaevskaya, L. Glascoe, and M. Singer, 2010: *High Resolution Atmospheric Modeling for Wind Energy Applications*. Lawrence Livermore National Laboratory Report LLNL-TR-426095, Livermore, CA
5. Wilber, D.; Daigler, D.; Nielsen, E.C.; Riedhauser, S.R.; Shanks, A.; Thompson, R.C.; Nasstrom, J.S., 2007: Nuclear/radiological emergency response in the USA, *Int. J. Emergency Management*, **4** (3), 339-55
6. Homann, S., 2011: *HotSpot v2.07.2 User's Guide*, Lawrence Livermore National Laboratory Report, Livermore, CA
7. Harper, F.T., S.V. Musolino and W.B. Wentz, 2007: Realistic Radiological Dispersal Device Hazard Boundaries and Ramifications for Early Consequence Management Decisions, *Health Physics*, **93**

8. Freiling, E.C., 1963: Theoretical Basis for Logarithmic Correlations of Fractionated Radionuclide Compositions, *Science*, **139**
9. Tompkins, R.C. *Department of Defense Land Fallout Prediction System – Volume V: Particle Activity*. Defense Atomic Support Agency, U.S. Army Nuclear Defense Laboratory, Edgewood Arsenal, MD, NDL-TR-102, DASA 1800-V, AD832239, February 1968
10. Spriggs, G.D., V. Jodoin, J.R. Furlong, 2008: *Livermore's Weapon Activation Code, LWAC: Quick Start User's Manual*, Lawrence Livermore National Laboratory, Livermore, CA, UCRL-SM-229671-Rev 5, December 1, 2008. OUO/Export Controlled.